

Characterisation of fs-laser written refractive index changes using Near-field Scanning Optical Microscopy

D.Little*^a, P. Dekker^a, A. Rahmani^b, J. Dawes^a, G. Marshall^a, M. Withford^a

^aCentre for Ultra-high bandwidth Devices for Optical Systems & MQ Photonics Research Centre, Macquarie University, North Ryde, NSW, Australia 2109;

^bCentre for Ultra-high bandwidth Devices for Optical Systems, University of Technology Sydney, Broadway, NSW, Australia 2007;

ABSTRACT

We have performed measurements using a purpose-built Near-field Scanning Optical Microscope and shown that waveguides written with a fs laser in the kHz regime have an asymmetry associated with the unidirectional nature of the writing beam. Further, the asymmetry becomes more pronounced with increasing pulse energy. At very high pulse energies (5-10 J) the presence of multiple guided regions was also observed, indicating that the refractive index profile of the waveguide possesses several maxima, a result which is consistent with current studies on the filamentation process that high-powered laser pulses experience in a dielectric medium. In this paper we will present these observations, their subsequent analysis and implications for photonic device fabrication using this method.

Keywords: Ultrafast Processing, Femtosecond waveguide, Near-field Optics, Near-field Microscopy.

1. INTRODUCTION

Direct-writing of waveguides in bulk glass using a femtosecond-pulsed laser has been shown to be versatile method by which compact photonic devices can be fabricated. The spectrum of devices that have thus far been demonstrated include evanescent couplers, 1 to N splitters and waveguide Bragg gratings in passive glass, while waveguide amplifiers, external cavity lasers and monolithic distributed Bragg reflector lasers have been demonstrated in active glass¹⁻⁴.

Device fabrication using this method is based on the multi-photon absorption mechanism when a femtosecond laser pulse is focused inside a bulk dielectric medium such as glass. The interaction between the laser pulse and the dielectric medium is known to be a highly nonlinear process, involving plasma generation, plasmon interactions and beam filamentation. Under the right conditions, this mechanism can lead to a permanent refractive index change that is localized at the point of interaction. While many studies have been done on the interaction between the femtosecond laser pulse and a dielectric medium, only in the last couple of years have researchers examined higher-order structure within the induced refractive index profile and its effect on the optical properties of waveguides fabricated using this method⁵.

To characterize the optical properties of fs-written waveguides, a purpose-built Near-field Scanning Optical Microscope (NSOM) was used. Near-field Scanning Optical Microscopes are unique in that they are able to detect evanescent waves. As a result, NSOMs able to achieve spatial resolutions better than that allowed by the far-field diffraction limit, as they are able to measure the true optical near-field before it evolves into its far-field form, the evolution of which occurs over just a single wavelength of propagation which necessitates the need for the NSOM probe to be positioned very close ($< \lambda$) to the source⁶. In addition, they remain the only means by which light propagating *within* a photonic device can be measured, through the detection of the evanescent component of a guided wave.

The motivation for this study was to shed some light on two veritable unknowns regarding fs-laser written waveguides. Firstly, the exact shape of the fundamental mode as it propagates down the waveguide. Detailed knowledge of the mode profile of these guides will assist in developing better techniques for efficiently coupling light in and out of these devices, something that is currently a problem for researchers. The other unknown is the exact refractive index profile induced by the aforementioned method for obtaining a permanent, localized refractive index change. It is often assumed

that the index profile induced by this method is similar to that of an optical fibre, however it has emerged from material studies that this is unlikely to be the case. Deviations from the refractive index profile of an optical fibre will have implications for waveguide geometries such as waveguide bends and devices that rely on evanescent coupling.

2. METHODOLOGY

2.1 Femtosecond direct-writing of waveguides in fused silica

Waveguide samples were fabricated using a Hurricane Amplifier/Oscillator system which runs at a wavelength of 800 nm, a pulse repetition rate of 1 kHz and has a pulse width of approximately 100 fs. A range of pulse energies were used ranging from 3.5 J to 10 J. The beam was focused using a 20x objective and the focus was located 100 μ m below the glass surface. The fused silica block was translated through the focus at a rate of X m/s. The fused silica sample is then post-processed by grinding back and polishing both end facets using a Logitech grinder & polisher.

One fused silica block was further processed by grinding and polishing down the top facet at an angle of $\sim 2^\circ$. A fibre was then pigtailed to the input facet of this sample using a piece of ferruled fibre glued to the waveguide input using Norland 63 UV-curable epoxy.

2.2 Near-field Scanning Optical Microscope

A basic Near-field Scanning Optical Microscope was constructed by mounting a tapered optical fibre NSOM probe on a quartz tuning fork with a resonance frequency of 32.768 kHz to a piezoelectric actuator. The piezoelectric actuator was driven using the internal oscillator from a Stamford SR830 lock-in amplifier, and the resulting amplitude of vibration from the probe/tuning fork resonator (which had a resonance frequency of 30-32 kHz when combined) could be monitored using the lock-in amplifier. The purpose of monitoring the vibration amplitude is to detect the shear-force the probe experiences as it is brought to within ~ 100 nm of a surface, which is an accurate means by which the distance between the probe and sample can be monitored.

Positioning and motion control of the probe was achieved using a pair of 6-axis Melles Griot Nanomax stage. Each axis on the Nanomax possesses a piezoelectric actuator and a feedback sensor system that yields a positional resolution of 5 nm. The NSOM head was affixed to a separate piezoelectric actuator that possessed a positional resolution of < 1 nm. Motion control was achieved by programming the voltage pre-amplifiers that control the piezoelectric actuators. The stage was programmed to scan a target surface in a raster fashion, and could take around 30 measurements per second.

2.3 Light Sources and Detectors

Waveguides were probed using a JDS Uniphase 1550 nm Swept-Wavelength-Source (SWS) for output face measurements and a HeNe 633 nm fibre coupled laser source for evanescent field measurements. The maximum power of the SWS was 4 mW while the maximum power of the HeNe fibre-coupled source was around 8 mW. Both sources were very stable over long time periods, and were chosen for this reason.

Light at 1550 nm was detected using a fibre-coupled InGaAs PIN photodiode. Measurements from the InGaAs photodiode were compiled using LabView via a Stamford Sr245 Computer Interface module. Red 633 nm light was chopped at 200 Hz and detected using a Photomultiplier Tube (PMT) biased at 1300 V. Measurements using the PMT were read directly from a CRO and averaged over 32-256 traces.

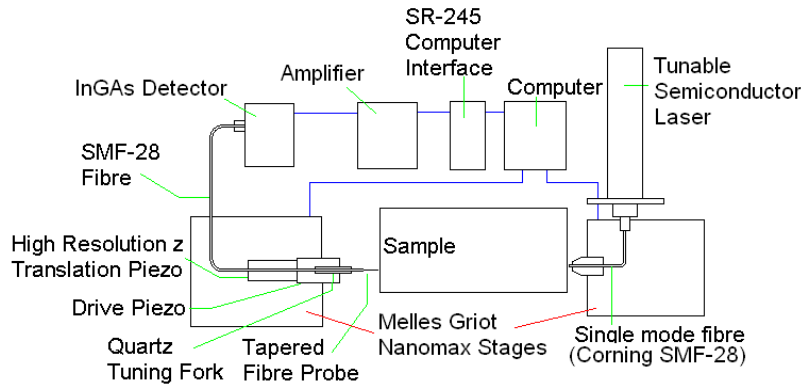


Fig. 1. Experimental layout for end-on measurements of a fs-written waveguide using a NSOM probe at a wavelength of 1550 nm. Stage control and data compiling was done using LabView.

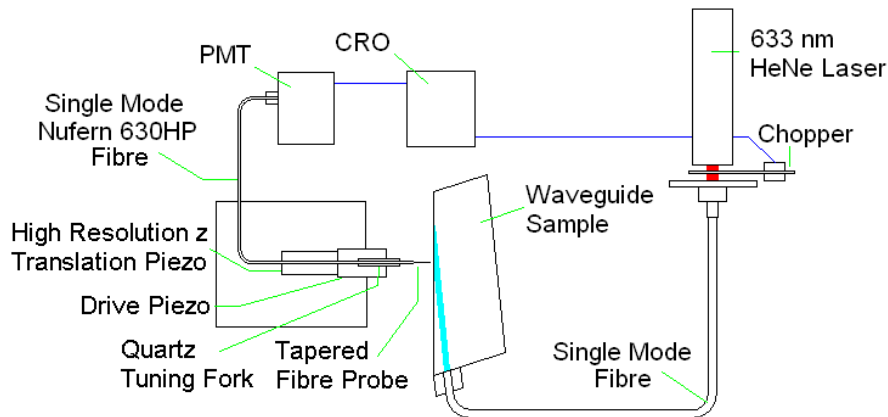


Fig. 2. Experimental layout for evanescent measurements of a fs-written waveguide using a NSOM probe at a wavelength of 633 nm. Stage control and data compiling was done manually.

3. RESULTS

3.1.1 Measurement of the output mode of a fs-written waveguide @ 1550 nm.

Using the setup depicted in figure 1, the following images were taken of the output mode of waveguides written with varying pulse energies. From the reference frame defined by the orientation of the scan axes, the writing laser beam comes in from the right hand side and propagates horizontally toward the left during waveguide fabrication. The NSOM itself was calibrated by imaging the output mode of an optic fibre with a known mode-field diameter. The resolution of the NSOM probes was ~ 300 nm, and images were taken with a step size of 300 nm between measurements.

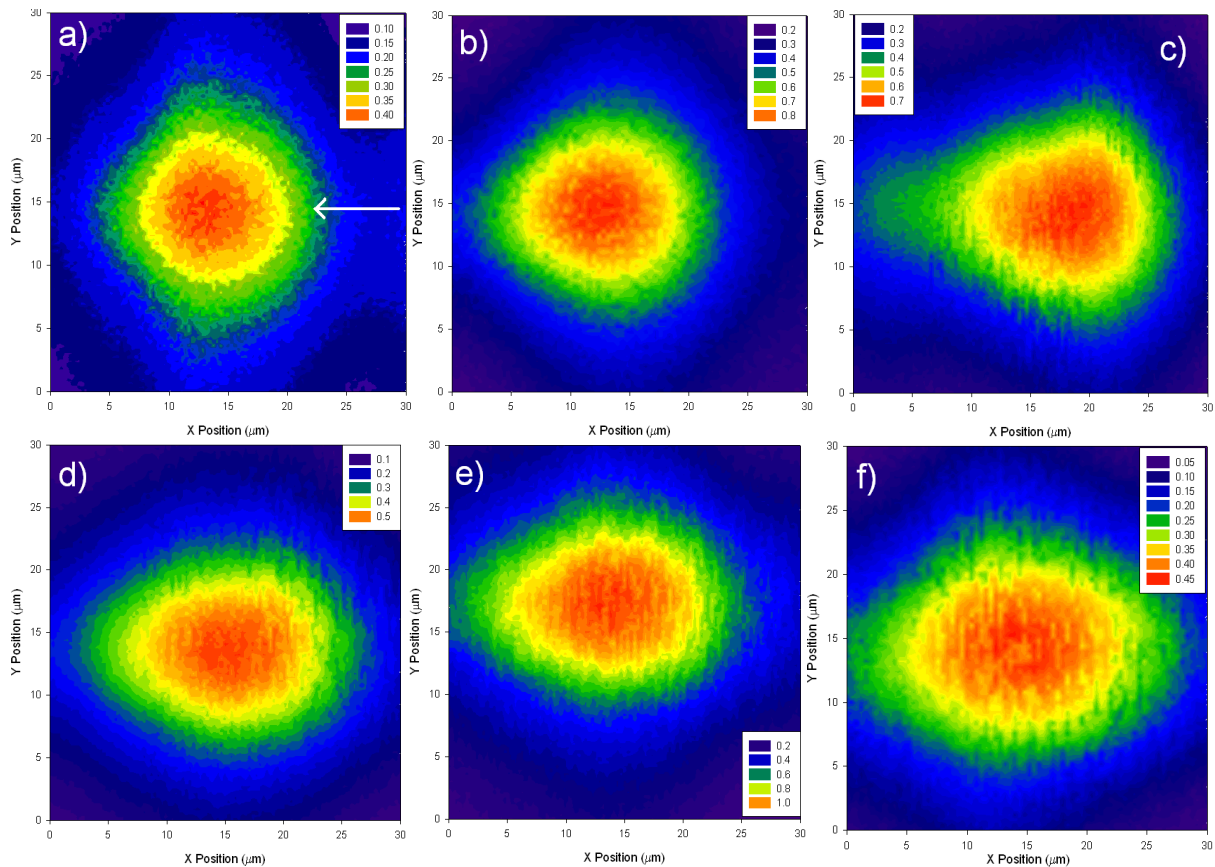


Fig. 3. Images taken using NSOM of the output mode of waveguides written in fused silica with pulse energies of a) 3 J, b) 3.5 J, c) 4 J, d) 4.5 J, e) 5 J, f) 10 J. The white arrow in a) denotes the direction of the writing beam.

There are two points of interest to be taken from the images in figure 3;

- Elongation of the output mode in the direction of the writing beam as the pulse energy of the writing laser is increased. Waveguides that possess an elliptically shaped mode are undesirable due to the difficulty of attempting to mode-match such waveguides to fibre modes, thus coupling to such modes using fibres, one would expect to see greater input and output coupling losses. Waveguides written with higher pulse energies have been shown to be optimal in terms of propagation loss, however in terms of coupling losses, lower pulse energies (around 3 J) appear to be optimal, judging by the shape of the resultant output mode.
- Asymmetry of the waveguide mode about a vertical axis. It is well understood that the writing beam is asymmetric along its Rayleigh range due to nonlinear effects such as self-focusing, however the implications of this on the resultant refractive index profile of the waveguides and the shape of the fundamental mode is still relatively unknown. Images in figure 3 suggest that there is an asymmetry in the mode present, which manifests as an elongated “tail” on the left hand side of the mode profile. This feature is most prominent in figure 3 c), however it is present in all guides to varying degrees. While it is possible to shape the beam such that a symmetric central region is obtained, such as that obtained in figure 3 a) and to a lesser extent, 3 b), the asymmetry persists in the outlying mode regions.

Figure 3 therefore suggests that the refractive index profile of these waveguides is not cylindrically symmetric, even for guides that have a central symmetric region. This has implications for more complex waveguide geometries that rely on this symmetry in the refractive index for normal operation such as bends, splitters and

couplers. Bends that bend in different directions for example would possess different mode profiles even if they possess the same radius of curvature.

While there is asymmetry along the length of the Rayleigh Range, symmetry is preserved about the axis of the writing beam. Therefore the aforementioned effects due to asymmetry in the refractive index profile would not be expected to significantly affect 2D circuits.

3.1.2 Variation in output mode profile with input mode

The above experiment was repeated except the input fibre was moved by 5-10 μm and the resultant images were compared to the measured profiles with the position of the input fibre unperturbed.

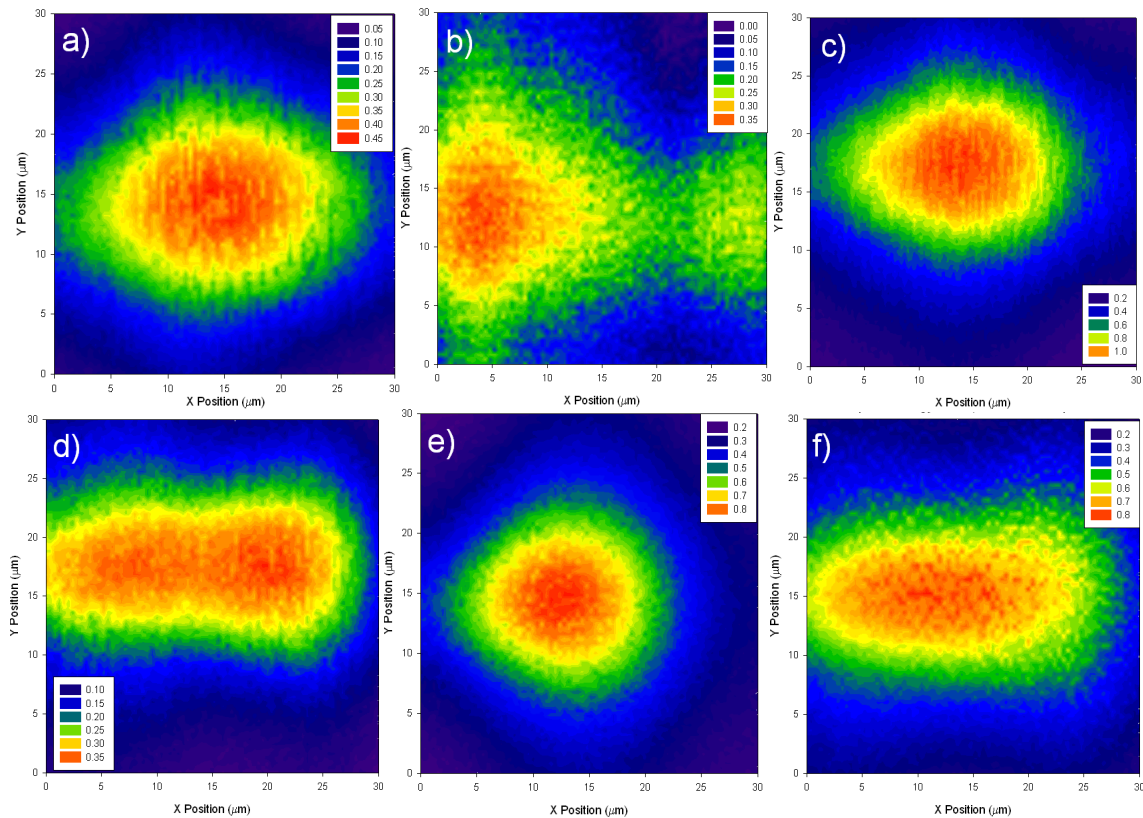


Fig. 4. Images taken using NSOM of the output mode of waveguides written in fused silica written with pulse energies of a) 10 J, c) 5 J, e) 3.5 J, and images of the output mode taken with the input beam offset by 5-10 μm in the direction of the writing beam, for waveguides written using pulse energies of b) 10 J, d) 5 J and f) 3.5 J.

Ordinarily, say in a fibre for example, one would not expect the profile of the output mode to vary with the input, one would only expect the total power within the mode to vary. This was observed not to be the case with fs-written waveguides. Two factors are thought to contribute to this first, the length of each waveguide is only 5 mm or so, and second, the refractive index contrast between the core and cladding region is small, typically only 1×10^{-3} . These two factors contribute to result in leaky modes – modes that ordinarily decay exponentially along the length of the waveguide – persisting along the full length of the waveguide. What is interesting is not so much the presence of leaky modes at the output per se, but the resultant output mode profile due to these leaky modes.

Not only is the mode profile drastically different when the input beam is offset by 5-10 μm in the direction of the writing beam, there is evidence of a second maximum present in waveguides written with higher pulse energies. At waveguides written at pulse energies below 4.5 μJ , there is no second maximum evident, however the mode is significantly elongated in the direction of the writing beam.

These measurements reveal to some extent the complexity of the refractive index profile induced by the writing beam, particularly at higher energies. There are two possible causes of a second maximum, either there are higher order modes present, which would imply that the core region is somewhat larger than the images in figure 3 would seem to imply. The other possibility is that there are multiple maxima in the refractive index profile, the presence of which is masked when the alignment is optimized by launching the input mode in between the two refractive index maxima.

3.2 Evanescent wave measurements of a fs-written waveguide with an angled air-glass interface

To investigate the optical properties of these waveguides further, a glass sample containing a fs-written waveguide was polished down so that the air/glass interface intersected the waveguide itself. Polishing the sample back in this way allows access to the evanescent portion of the propagating wave, which NSOM is ideally suited to measure.

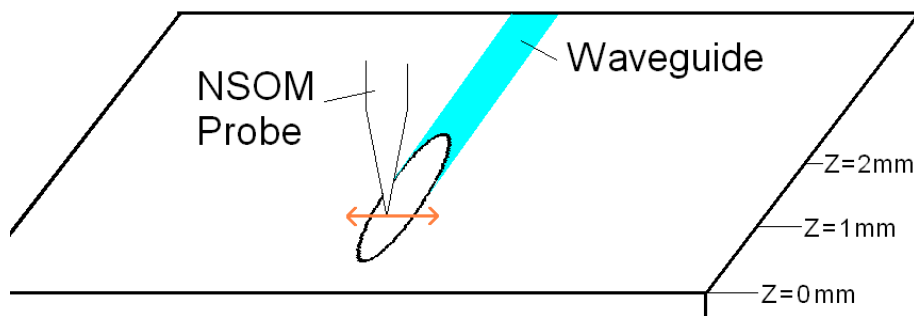


Fig. 5. An illustration of how the evanescent field profiles were measured.

Measurements of the evanescent field profile using the setup depicted in figure 2 were made every 100 μm along the length of region where the polished air/glass interface intersected the fs-written waveguide. Individual measured evanescent field profiles were then compiled to make a 2D cross-sectional image of the evanescent field.

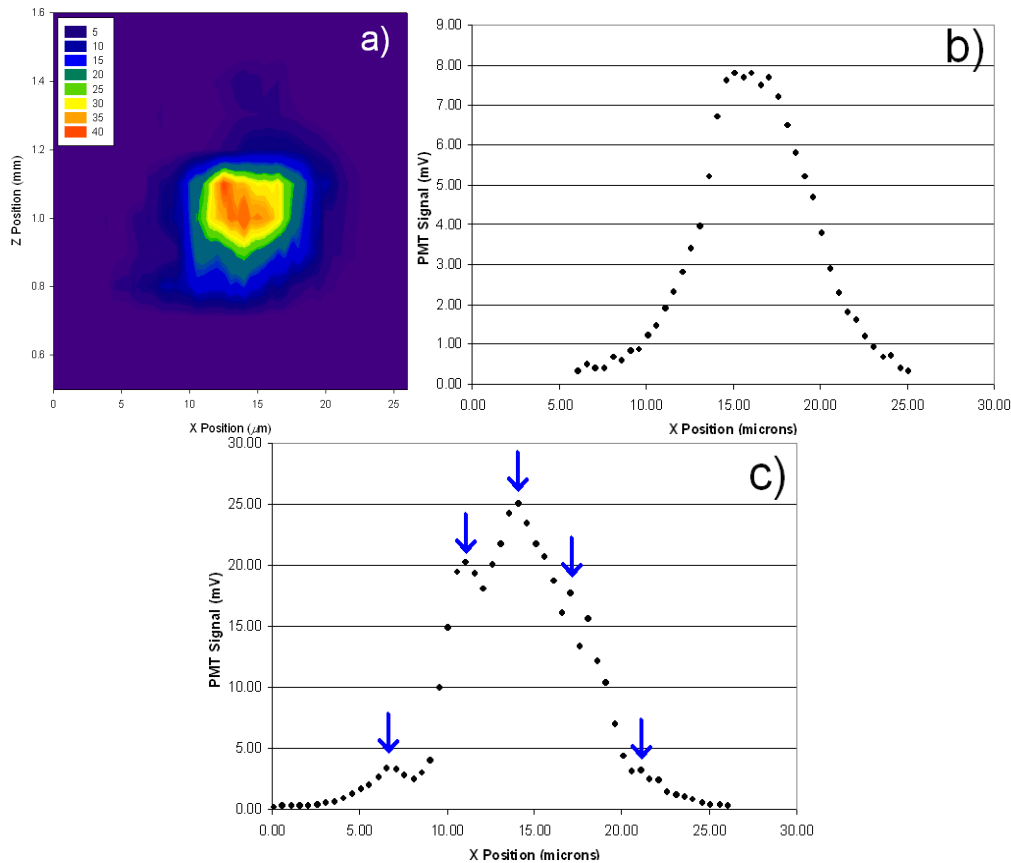


Fig. 6. a) 2D profile of the evanescent field at the intersection of the waveguide and the air/glass interface. The Z position on the vertical axis refers to the position along the intersection region the cross-sectional scan took place. The zero reference of the Z position was taken to be the edge of the waveguide sample, b) The measured evanescent field profile at $Z = 1.2$ mm, and c) The measured evanescent field profile at $Z = 0.9$ mm. Arrows highlight the peaks in the measured field profile.

Two distinct trends are evident in figure six, firstly the profiles that were measured above the central mode region, such as that shown in figure 6 b) are much better Gaussian fit that those measured below the central mode region such as that shown in figure 6 c). Secondly, there is strong asymmetry in the vertical direction; the “tail” at the lower end of the image is much longer than the tail at the upper end of the image.

From the ray model of wave propagation, it is predicted that light will totally internally reflect at the angled interface and, if the air/glass interface is steep enough, couple out of the waveguide altogether. There is however a consideration that complicates this simplified picture, namely the potential for the cross section between the waveguide and the air/glass interface to behave as a tapered waveguide. The effect of this would be to cause the detected field to “smear out” in the vertical direction. A quick calculation can confirm that no such smearing is present, simply by transforming the Z coordinate into a Y coordinate via the following equation;

$$Y(\mu\text{m}) = Z(\mu\text{m}) \times \tan(2^\circ)$$

From figure 6 a), the central maximum extends over 200 ± 20 μm in length, which, using the above equation equates to a mode diameter of 6.8 ± 0.7 μm which matches up well with the observed mode diameter along the X direction in figure 6 a). A case can therefore be made that the long tail at the bottom of the image in figure 6 a) is not an artifact due to the intersected region acting like a waveguide taper, but genuinely a result of the optical properties of the unperturbed waveguide.

The remaining point of note is the presence of higher-order structure in the measured mode toward the lower portion of the waveguide. The presence of multiple maxima in the measured profile suggests, as with the previous set of experiments that multiple refractive index maxima exist, or at the very least, the refractive index profile is not a simple, cylindrically symmetric step-index or Gaussian profile that is normally assumed to be the case.

One mechanism that has been reported in literature is the formation of nano-structures caused by the presence of electromagnetic standing waves during the refractive index modification process⁷. The position and separation of the maxima of the measured evanescent field in figure 6 a) however is inconsistent with the refractive index profile generated via this mechanism.

Another suggested mechanism by which these multiple refractive index maxima come about is the filamentation that the writing beam experiences when focused inside a dielectric medium. Filamentation occurs when the power of a laser beam is several times the critical threshold for self-focusing. When this occurs, defocusing of the laser beam due to plasma generation (which in turn is a result of multi-photon absorption) balances the self-focusing, and the beam propagates as a solution-like "filament". If the power of the laser is sufficient, the beam will split into several filaments, a phenomenon known as multiple filamentation.

Kudriasov et al.⁸ showed that multiple filamentation should arise when the pulse energy exceeds about 2 J. As the waveguide sample probed in figure 6 a) was written with a pulse energy of 3 J, it is expected that filamentation of the writing beam occurred during the fabrication process. The modeling of Kudriasov et al. shows that waveguides written with energies with pulse energies from 2.4 – 5.0 J should possess a structure that has a main central filament, with a secondary filament either side of this central filament, with each secondary filament spaced ~1.5 times the width of the central peak from the centre of the beam profile.

From figure 6 a) and 6 c), judging from the position of the secondary peaks in the detected evanescent field that occur either side of the centre of the beam profile toward the lower end of the measure field profile, the filaments that generated the refractive index maxima responsible for these secondary peaks would have to have been spaced roughly 8 m apart, which would imply a central beam spot of 3-3.5 m, which is consistent with the laser parameters used to fabricate these waveguide samples. We therefore conclude that filamentation of the writing beam is responsible for the presence of secondary maxima in the measured evanescent field profile of a fs-written waveguide polished back at a slight angle.

4. CONCLUSION

We have compiled evidence using a Near-field Scanning Optical Microscope that fs-written waveguides do not possess a cylindrically symmetric step-index or Gaussian refractive index profile as is usually assumed to be the case. The output modes of a series fs-waveguide samples were found to possess mode profiles that would not be expected if the refractive index profile was cylindrically symmetric, in addition, when the input fibre was displaced, the shape of the output modes changed dramatically; something which is thought to be a result of leaky modes persisting throughout the entire length of the waveguide and having a measureable effect at the output. The shape of these leaky modes possessed several maxima which we believe hints at a more complex refractive index structure.

Further evidence was obtained by polishing back a fs-waveguide sample at a slight angle, intersecting the waveguide contained within and allowing us to measure the resultant evanescent field. The measured profiles of the evanescent field, when compiled, revealed the existence of a long tail after the central peak, as well as higher-order structure within this tail. Beam filamentation of the writing beam is proposed as the mechanism that causes this structure to arise.

REFERENCES

¹ K. Minoshima, A. M. Kowalewicz, E. P. Ippen and J. G. Fujimoto, "Fabrication of coupled mode photonic devices in glass by nonlinear femtosecond laser materials processing", *Opt. Express* **10**, 645-652 (2002).

² G.D. Marshall, M. Ams and M. J. Withford, "Direct laser written waveguide Bragg gratings in bulk fused silica", *Opt. Lett.* **31**, 2690-2691 (2006).

- ³ R. Osselame, N. Chiodo, G. Della Valle, G. Cerullo, R. Ramponi, P. Laporta, A. Killi, U. Morgner and O. Svelto, "Waveguide lasers in the C-band fabricated by laser inscription with a compact femtosecond oscillator", IEEE Journal of selected topics in Quantum Electronics **12**, 277-285 (2006).
- ⁴ G. D. Marshall, P. Dekker, M. Ams, J. A. Piper and M. J. Withford, "*Monolithic Waveguide-Laser Created Using the Direct Write Technique*", *Postdeadline Paper JWBPDP2 in Bragg Gratings, Photosensitivity and Poling in Glass Waveguides (BGPP)*, Quebec, Canada, 2007.
- ⁵ K. M. Davis, K. Miura, K. Hirao, "Writing waveguides in glass with a femtosecond laser", Opt. Lett. **21**, 1729-1731 (1996).
- ⁶ R. C. Reddick, R. J. Warmack, and T. L. Ferrel, "New form of scanning optical microscopy", Physical Review B **39**, 767-770, (1989).
- ⁷ Y. Shimotsura, P. G. Kazansky, J. Qiu, K. Hirao, "Self-Organised Nanogratings in Glass Irradiated by Ultrashort Light Pulses", Phys. Rev. Lett. **91**, 247405, (2003).
- ⁸ V. Kudriasov, E. Gaizauskas, V. Sirutkaitis, "Beam transformation and permanent modification in fused silica induced by femtosecond filaments", J. Opt. Soc. Am. B **22**, 2619-2627, (2005).